10th ANKARA INTERNATIONAL AEROSPACE CONFERENCE
18-20 September 2019 - METU, Ankara TURKEY

AIAC-2019-206

UNSTEADY REYNOLDS AVERAGE NAVIER-STOKES AND DETACHED EDDY SIMULATIONS OF TRANSONIC CAVITY FLOWS

Seyfettin Coşkun* and Yusuf Özyörük†
Middle East Technical University
Ankara, Turkey

ABSTRACT

High speed flow past an open (deep) cavity consists of highly unsteady aerodynamic phenomena. Understanding its physics and simulation is crucial for the cavity design. Highly turbulent and complex nature of cavity flow phenomenon requires use of scale resolving turbulence models such as Large Eddy Simulation (LES). In literature, scale resolving approaches appear to be employed increasingly in cavity flow and noise predictions, but they are still expensive for routine use in design environment. Unsteady Reynolds Average Navier-Stokes (URANS) models, on the other hand, lack of resolving the turbulence structures. Lower computational costs of URANS models deserve investigation for applicability on cavity flow solutions. An alternative to LES and URANS methods is the Detached Eddy Simulation (DES), which utilizes both URANS and LES. DES has lower computational costs than LES and improved flow physics than URANS. In this paper, Unsteady Reynolds Average Navier-Stokes (URANS) and Detached Eddy Simulation (DES) methods are utilized for initial studies. Particularly flow and acoustic predictions of the M219 rectangular clean cavity (no doors, stores etc.) are carried out. Although, URANS methods are not impeccably suited for acoustic noise prediction purposes due to its averaging nature, it is shown in this work that URANS methods can closely predict cavity noise levels and frequency content of an open cavity, M219, when meshing is done suitably. It is also shown in the present work that DES methods properly capture the flow physics and noise environment of M219 cavity.

INTRODUCTION

Cavity flows are encountered in many engineering applications such as aircraft landing gear housings and weapons bays. High speed cavity flows are basically characterized by unsteady compressible aerodynamic phenomena such as flow separation, shear layer instabilities, vortex shedding, self-sustained flow oscillations, and etc. [Pereira and Sousa, 1995; Rossiter, 1960; Stallings and Wilcox, 1960; Zhang and Edwards, 1990]. Cavity flows consist of open, closed, and transitional flow types depending on the cavity geometric parameters, length-to-depth (L/D) ratio constitutively [ESDU, 2004; Plentovich and Stallings and Tracy , 1993]. In closed cavity flows ($L/D > 13$), separated flow penetrates into the cavity, causing large gradients in the pressure distributions along its baseline. In the weapons bay cases this may impose undesired pitching moment on the store content, which is in turn vital

*Student in Dept. of Aerospace Engineering, Email: seyfettin.coskun@metu.edu.tr
†Professor in Dept. of Aerospace Engineering, Email: yusuf.ozyoruk@metu.edu.tr

to its separation characteristics from the bay. In open cavity flows ($L/D < 10$), on the other hand, separated flow forms a highly unsteady shear layer across the cavity opening which reattaches on the trailing edge. Acoustic waves are generated at the trailing edge, propagating upstream within the cavity which forms a feedback mechanism [Colonius and Rowley and Basu , 2002]. This causes high intensity acoustic spectrums in the open cavity flows [Lawson and Barakos , 2011; Rizzetta and Visbal, 2015]. Closed cavity flows are profitable in terms of acoustic environment of a cavity whereas open cavity flows are advantageous for store separation from aircraft weapons bays in terms of rather smooth pressure distribution along the cavity baseline. Transitional cavity flows $(10 < L/D < 13)$ exhibit both open and closed cavity flow characteristics depending on the geometric parameters [ESDU, 2004; Plentovich and Stallings and Tracy , 1993; Rossiter, 1960].

In previous research on high speed cavity simulations, scale resolving turbulence models, such as Large Eddy Simulation (LES) and Detached Eddy Simulation (DES) appear as the preffered approaches in predicting the cavity noise. These methods rely on resolving turbulence scales of the complex cavity flow rather than using statistical modelling [Rizzetta and Visbal, 2015], because the small scale eddies present in the unsteady shear layer have a critical effect on the generation of acoustic waves. In LES, significantly lower portion of the flow is modelled compared to URANS methods, which proves the accuracy of the LES. However, LES is still expensive for high Reynolds number flows [Nayyar and Barakos and Badcock , 2005].

DES is a hybrid method which takes advantage of URANS methods within the boundary layer region and LES in regions outside boundary. Advantage of DES methods over the LES methods is computational efficiency because of employing URANS methods in the wall regions Nayyar and Barakos and Badcock [2005]

URANS methods, on contrary to LES method, use fully statistical models rather than scale resolving. This brings the drawback of loss of accuracy in cavity noise predictions. However, URANS methods are not a complete scratch but they have a level of accuracy in prediction of cavity noise. This proposes to determine the availability of URANS methods for cavity configurations.

In the present study, a clean cavity (no doors, stores and etc.) is studied to simulate the flow field with use of $k-\omega$ SST and RNG $k-\epsilon$ URANS models along with improved delayed DES (IDDES) basically. Accurate simulation of a clean rectangular cavity is important before moving onto complicated cavity configurations.

METHOD

1 CFD Validation Test Case: M219 Cavity

M219 test cavity is utilized as a validation case to assess the suitability of various flow solvers available in the commercial FLUENT code for cavity flow solutions. Investigated CFD methods cover $k-\omega$ SST and RNG $k-\epsilon$ URANS models, and S-A DES, S-A DDES, and $k-\omega$ SST based IDDES methods. Ross [1997] conducted wind tunnel tests for the clean M219 configuration. M219 test case is an open type cavity with $L/D = 5$ and $W/D = 1$. It has $L = 0.508$ meters and $W = D = 0.1016$ meters dimensions, as shown in Fig. 1. Operating conditions for the test section are $M = 0.85$, $T = 251.77\ K$, $\mathrm{Re} = 6.7 \times 10^6$, $P = 63.1\ kPa$ Ross [1997].

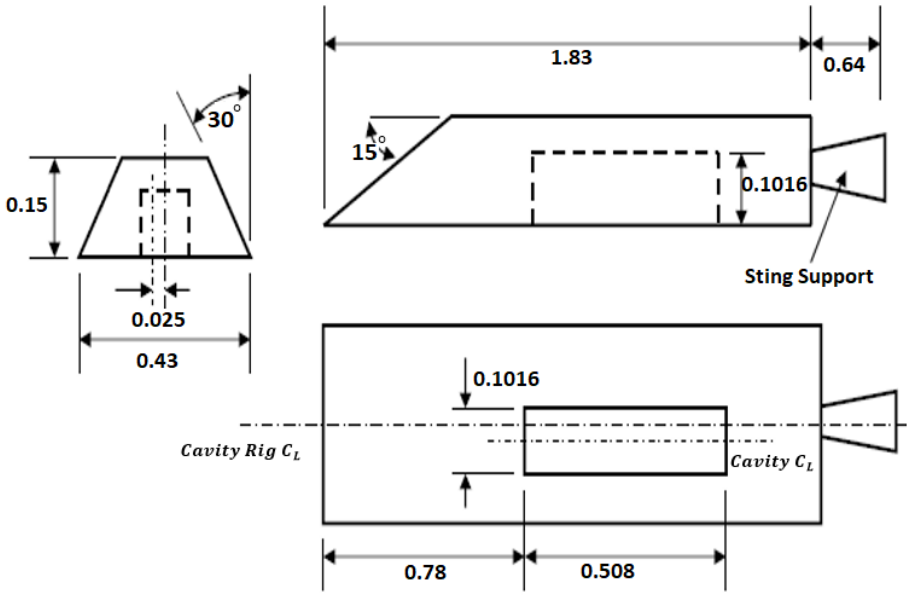

Figure 1: Experimental rig of M219 cavity model (dimensions in meters, adapted from Nayyar and Barakos and Badcock [2005])

In the experiment conducted by Ross [1997], 10 pressure tabs were located at the cavity centerline on the cavity ceiling, starting from $x/L = 0.05$ and located at equi-distance, as illustrated in Fig. 2. At each of these pressure tabs, instantaneous pressure was measured and post-processed to obtain OASPL and root-mean-square pressure levels, which are the indicators of the acoustic field in the cavity.

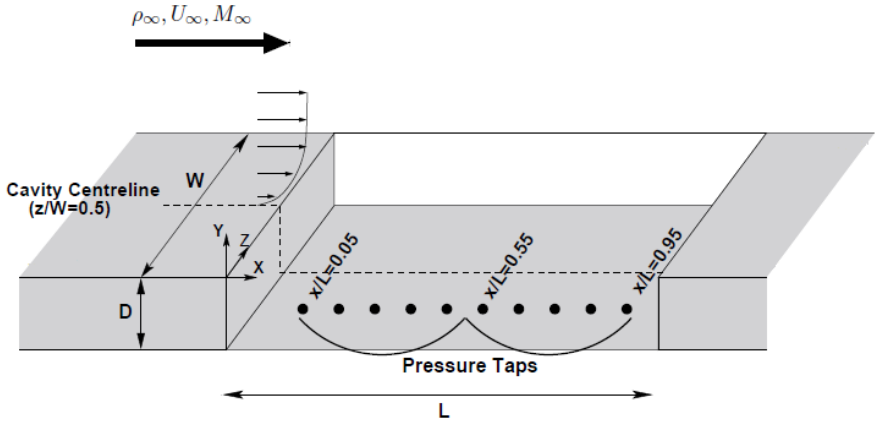

Figure 2: Locations of pressure tabs at the M219 test cavity baseline Nayyar and Barakos and Badcock [2005]

The M219 test cavity is selected for the computational study with the aforementioned turbulence models. The cavity configuration has a length-to-depth ratio of $L/D = 5$, and width-to-depth ratio of $W/D = 1$. A sample unstructured solution domain is illustrated in Fig. 3. The computations are conducted at a Mach number of 0.85, and Reynolds number of 6.7×10^6 based on the cavity length (0.508 m). In the computations, both Unsteady Reynolds Average Navier-Stokes (URANS) models and Detached Eddy Simulation (DES) methods are utilized.

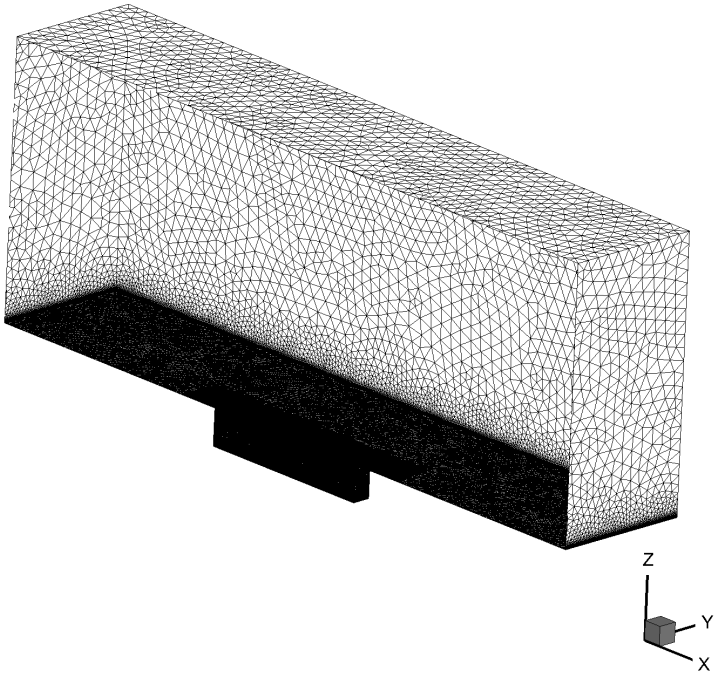

Figure 3: Sample computational domain for M219 geometry

RESULTS AND DISCUSSION

URANS Models in Cavity Flow Solutions

Complexity of cavity flows requires higher order scale resolving turbulence treatment such as application of LES, DNS and etc. However, because of high computational burden of LES and DNS methods, researchers still desire to benefit from methods with lower costs and acceptable accuracy. URANS methods are examples to these alternative methods for cavity flow solutions. Although they are not impeccably suited for acoustic noise prediction due to their averaging and modeling nature, applicability of URANS models still deserves to be investigated for cavity flows. Hence, we in this section discover prediction capability of URANS with the k-ω SST and RNG k-ϵ turbulence models. The study is discussed in the next subsection.

Grid Independency:

First step into a CFD solution is to conduct a grid independency study to determine the minimum grid requirement for an acceptably grid independent solution. In particular, independency of the overall sound pressure level (OASPL) is checked here on the centerline of the cavity ceiling. A total of 5 different grids is considered with the grid size and solution parameters provided in Table 1. $y+$ in the table shows the dimensionless form of the physical thickness of the first layer of the mesh in the boundary layer (B/L). This parameter is a quite important because it directly affects the B/L resolution. General cell size distribution within the cavity is crucial in resolution of complex flow characteristics. On the other hand, grid size has a direct influence on the computational cost, and therefore the best compromise conditions should be established.

Table 1: Parameters for URANS Grid Convergence Study

	Grid 1	Grid 2	Grid 3	Grid 4	Grid 5
y+	1	0.5	0.667	0.3	0.667
First Layer Thickness ($\times 10^{-6}$ m)	2	0.9	1	0.6	1
Number of Layers in B/L	30	51	41	61	41
Cell Size within the Cavity [mm]	3.5	3	2	2	1.75
Grid Volume Size ($\times 10^6$)	8	20	19	26	24

Solution on each grid is obtained through the k-ω SST and RNG k-ϵ turbulence models as indicated earlier. The attained OASPL results are compared to the experimental results provided by Ross [Ross and Peto , 1997] in Fig. 4. It is evident from the comparisons that the URANS computations captured the general trend of OASPL along the centerline of cavity ceiling, as the grids were refined, in particular within the cavity volume (Grid3 and 4). The k-ω SST turbulence model yielded more accurate OASPL values, Fig. 4 than the RNG k-ϵ turbulence model.

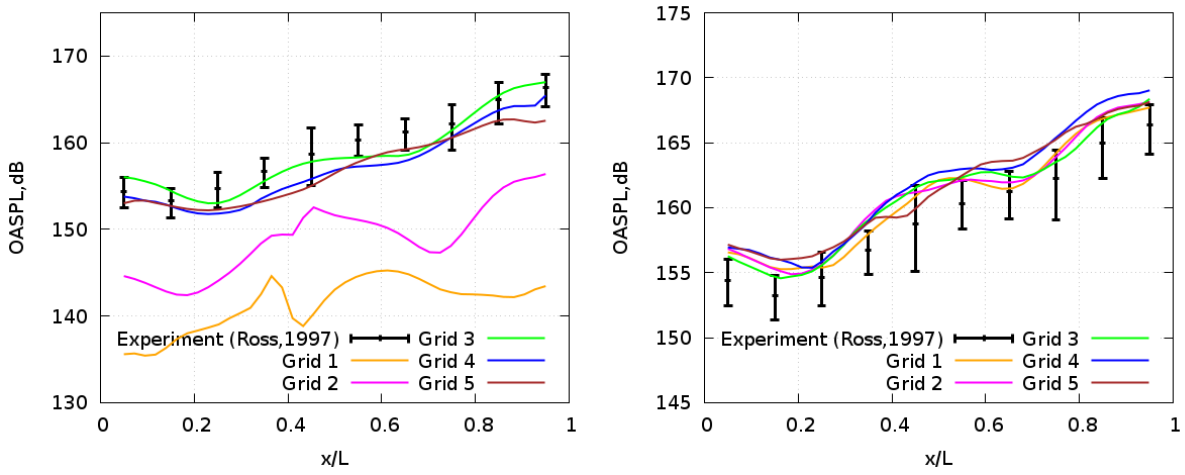

(a) k-ω SST model (b) RNG k-ϵ model

Figure 4: Results of URANS turbulence models for grid convergence study

It is interesting though to observe that the k-ω SST model yields results that have strong dependence on the computational grid, on the contrary to RNG k-ϵ model, which provides almost identical levels of accuracy for all of the grids used. The k-ϵ model yielded results on Grid 1 (coarse) not far from those on the other grids, while the k-ω SST model performed quite poorly on the same mesh. The mesh resolution, particularly in the vicinity of the walls and inside the cavity, seems to have their own distinct effects on noise predictions of cavity flows. Grid 3 predictions with the k-ω turbulence model seems the best among the others when compared to the measured data.

Another important aspect of the cavity flow fluctuations is their frequency distribution. The results for Grid 3 post-processed with Fast Fourier Transform (FFT) are shown in Fig. 5, for the root-mean-square pressure at the $x/L = 0.95$ point on the cavity ceiling. Experimental data of Ross [Ross and Peto , 1997] as well as analytically modeled Rositter frequencies are also included in the plot. It is evident that all the URANS computations, particularly those with the k-ω SST model, could predict the cavity dominant modal frequencies with reasonable accuracy. However, both turbulence models overpredicted the 2^{nd} and 3^{rd} modal amplitudes. Overprediction by the RNG k-ϵ model was less than that by the k-ω SST model. The 4th modal amplitude was missed almost entirely by the k-ω SST model, while RNG k-ϵ model had good prediction of it.

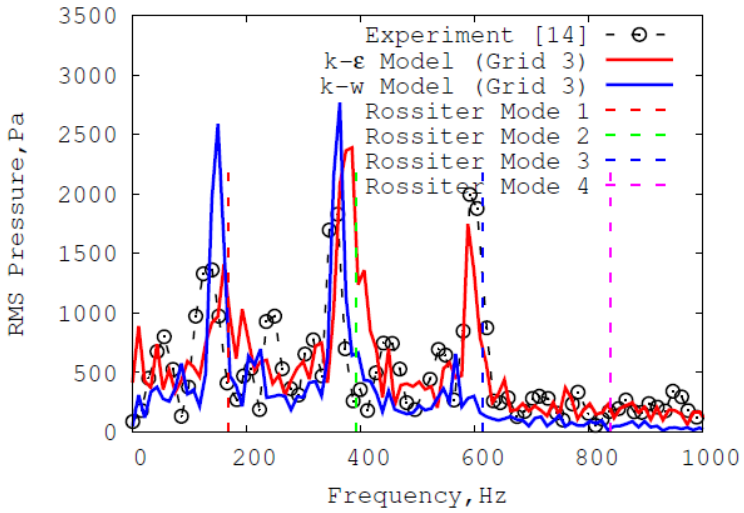

Figure 5: FFT obtained RMS pressure values at $x/L = 0.95$ point in comparison to Rossiter modes and experimental data.

Detached Eddy Simulations in Cavity Flow Solutions

Detached Eddy Simulation (DES) approach utilizes the best aspects of URANS and Large Eddy Simulation (LES) approaches, and is a widely accepted alternative solution method to cavity flows. The DES methods make use of URANS approach within the B/L, and LES elsewhere. Therefore, the DES methods are expected to provide improved results for cavity flow solutions. However, aforementioned issues existing in DES may have some hindering effects on the accuracy compared to URANS methods. DES with the Spalart-Allmaras (S-A) turbulence model, Detached DES (DDES) with S-A, and k-ω SST based Improved Detached DES (IDDES) methods are investigated in this section for the suitability to cavity flows.

Effects of Detached Eddy Simulation Variants: Results for OASPL and RMS pressure are shown in Fig. 6. It is clear that the DDES and IDDES methods yield OASPL with similar accuracy in Fig. 6a. DES, on the other hand, seems to perform poorly for the current problem. When Fig. 6 is analyzed more closely, it is seen that IDDES captures the peak fluctuation level, which occurs near the aft wall at $x/L = 0.95$, more accurately than the other approaches. IDDES also produced good comparisons for the entire length of the cavity in comparison to experimental data. Figure 6b shows that IDDES perfectly predicts both the modal frequencies and amplitudes of dominant modes in the pressure spectrum. DDES can predict the modal frequencies although it has a significant deviation from the modal amplitudes compared to IDDES in Fig. 6b. DDES closely estimates the frequency and amplitudes of some of the modes with significant deviations in magnitudes for some other modes. DES, on the other hand, performs the poorest results in terms of both OASPL and pressure spectrum in Fig. 6. Therefore, IDDES is considered as the most suitable model for the highly unsteady and turbulent cavity flow problems among the other detached eddy simulations variants considered here.

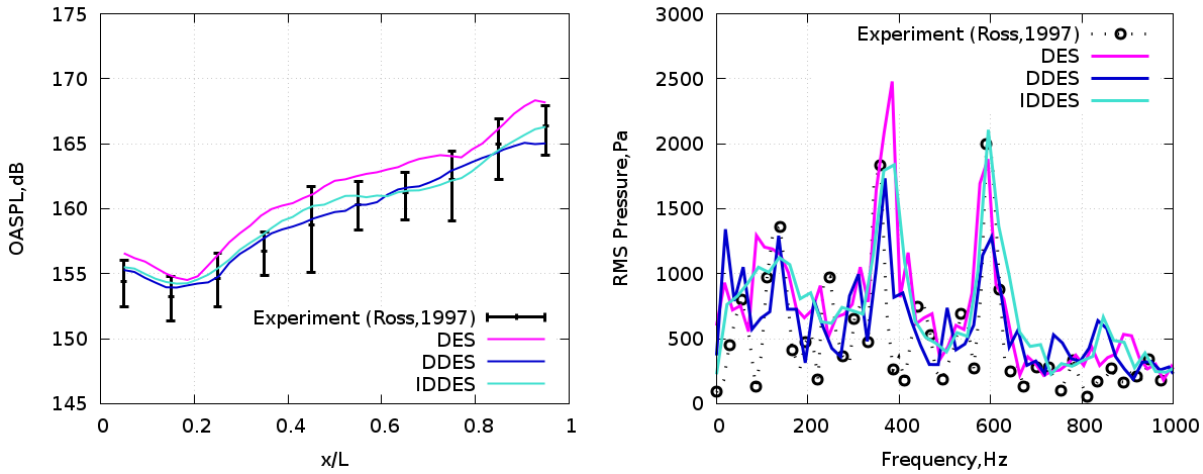

(a) OASPL (b) RMS Pressure at $x/L = 0.95$

Figure 6: Alternative DES methods predictions to cavity noise levels with experimental data ($M = 0.85$, $\Delta t = 1 \times 10^{-5}$ s) [Ross and Peto , 1997].

Detached Eddy Simulation Grid Independency: A grid convergence study is also conducted for IDDES method to determine the grid resolution that provides the highest computational efficiency without loss of accuracy. Since IDDES method utilizes URANS modeling approach within the boundary layer regions and LES outside, the best performing grid properties in URANS grid convergence study is utilized as the baseline grid (Grid 1-I). Only the grid size within the cavity (i.e. LES region) is refined such that the grid size is halved. Grid properties are shown in Table 2.

Table 2: Parameters for IDDES Grid Convergence Study

	Grid 1-I	Grid 2-I
Cell Size within the Cavity [mm]	2	1
Grid Volume Size ($\times 10^6$)	19	27

Results of the grid convergence study are compared in terms of both OASPL and frequency spectrum, as illustrated in Fig. 7. It is observed that further refinement of the cell size within the cavity does not have any significant effect on the accuracy of the simulations. Therefore, Grid 1-I is utilized in following simulations because of its computational efficiency without loss of accuracy.

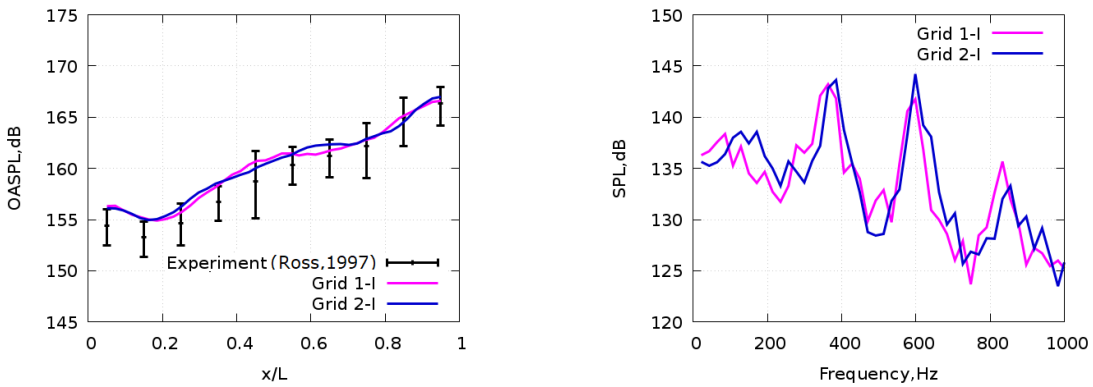

(a) OASPL (b) Pressure spectra at $x/L = 0.95$

Figure 7: Results of IDDES method grid convergence study ($M = 0.85$, $\Delta t = 1 \times 10^{-5}$ s)

An important parameter in solution of scale resolving turbulence models is the shear layer velocity profile. Instantaneous streamwise velocity data is collected at each time step throughout the simulation at constant x-lines along the centerline of cavity ceiling. Instantaneous velocity data is then averaged to compute the shear layer velocity profiles along the cavity, and it is compared to experimental data Barakos [2018] as shown in Fig. 8.

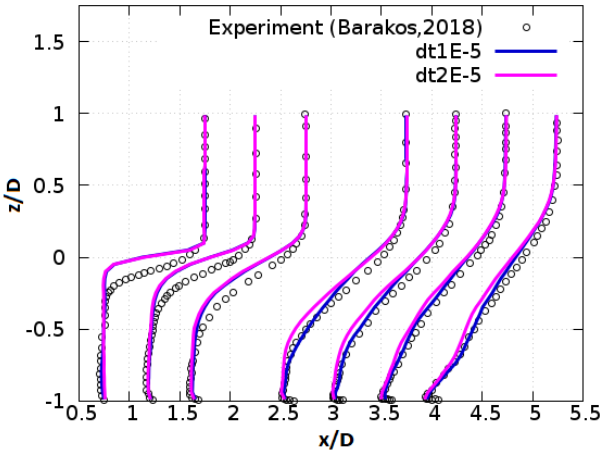

Figure 8: IDDES shear layer streamwise mean velocity profile compared to experimental data Barakos [2018]. The horizontal axis is scaled to $U/U_\infty + x/D$ ($M = 0.85$, $\Delta t = 1 \times 10^{-5}$ s)

It is evident from Fig. 8 that $\Delta t = 1 \times 10^{-5}$ s time step provides improvement in prediction of shear layer streamwise velocity distributions compared to $\Delta t = 2 \times 10^{-5}$ s, with increased accuracy towards aft of the cavity. However, in the front regions of cavity opening, where massive flow separation takes place, shear layer streamwise velocity profile predictions are not satisfactory for both time steps used. This could be attributed to the massive flow separation around the leading edge of the cavity that cause high gradients in the flow variables. In this region, IDDES model has difficulty because of the switching from URANS to LES mode.

Turbulence Models Comparison for Cavity Flow Solutions: In the present work, $k-\omega$ SST and RNG $k-\epsilon$ URANS models and DES, DDES, and IDDES methods are compared for related parameters to obtain the applicability of turbulence models of interest. Best performing URANS and DES methods are compared in Fig. 9.

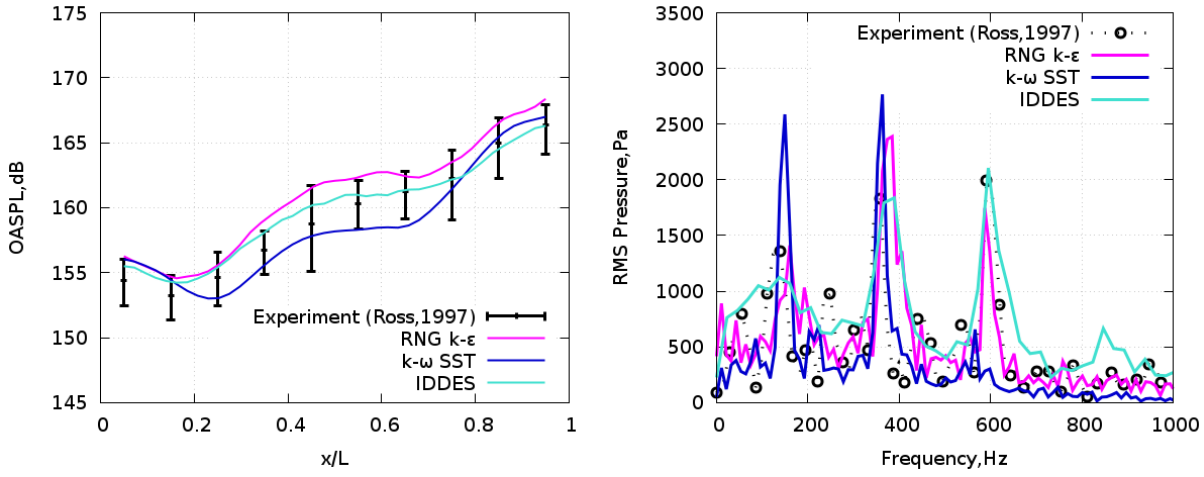

(a) OASPL (b) RMS Pressure at $x/L = 0.95$

Figure 9: Turbulence models comparison on cavity flow solutions

When Fig. 9 is analyzed more closely, it can be observed that IDDES is the best numerical method among the turbulent flow and acoustics solutions of cavity geometries. Although $k-\omega$ SST and RNG $k-\epsilon$ URANS models can predict the trend of OASPL along the centerline of cavity ceiling, IDDES performs far more better than URANS models in the prediction of cavity noise levels in Fig. 9a. When pressure spectrum is considered, superiority of IDDES method over URANS models is clear in Fig. 9b. Therefore, IDDES method is considered to be the best among utilized turbulence models. Flow features at various times are looked into closely. Fig. 10 shows instantaneous Mach contours at various fractions of the oscillation period T of the most dominant noise generating structures. For one period, T, of the dominant cavity mode (f ~ 600 Hz), cavity flow nearly completes a loop. Flow field at the starting time, t, and at the end of one period, $t+5T/6$, are quite similar to each other.

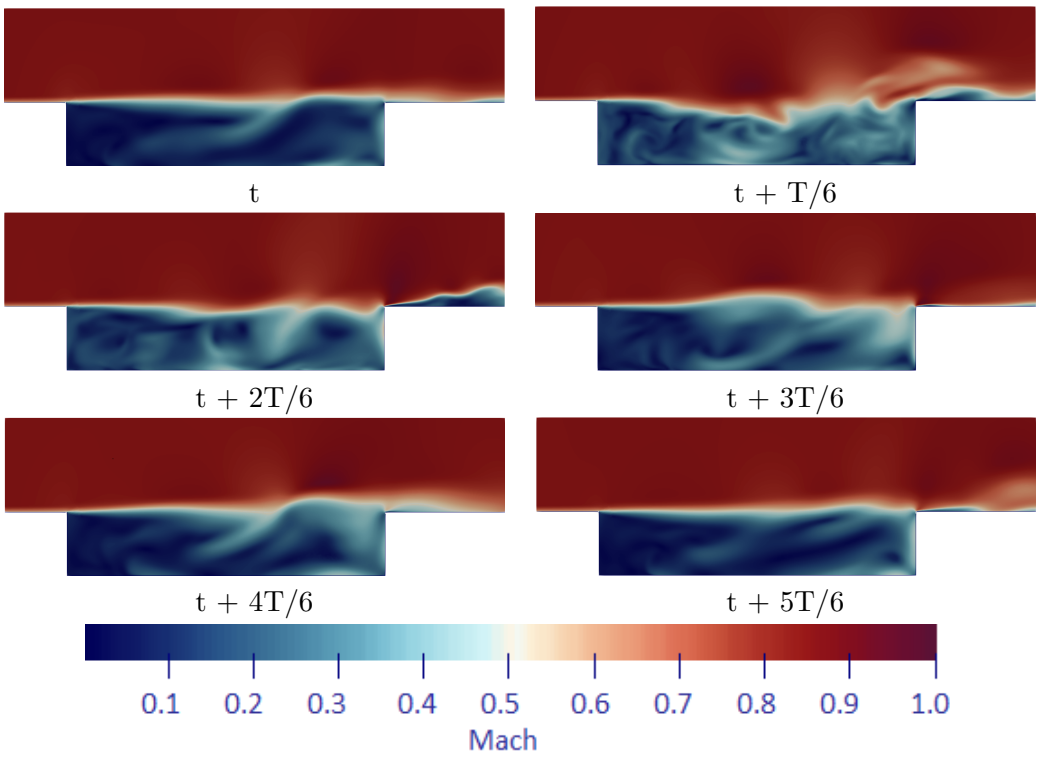

Figure 10: Instantaneous Mach contours at $1/6^{th}$ of period, T (0.00167 s), of the dominant mode (at $\sim$ 600 Hz).

It appears from the Mach contours that, despite the oncoming free stream Mach number is 0.85, local flow speeds go over Mach 1 along the shear layer, typical of transonic cavity flow situations. This, in turn, results in generation of shock waves that interact with the boundary layer and shear layer and contributes to the complexity of the flow. Unsteadiness and complexity of the cavity flow can be observed in Fig. 10. It can also be observed from the figure that cavity flow field is dominated by vortical flow structures that are extremely unsteady.

Further instantaneous flow visualizations are shown in Fig. 11 for the clean cavity configuration at the aforementioned spanwise offset planes. In flow visualizations, line integral convolution (LIC) technique is utilized. LIC is a technique that convolves a vector field to obtain streaking patterns which follow vector field tangents.

Flow visualizations in Fig. 11 on the offset planes demonstrate the 3-dimensionality of the flow field. There is a core vortex structure spanning over the cavity length accompanied by secondary vortical flows at the corner regions in all of the offset planes. It is observed from Fig. 11 that the extent and locations of the vortex structures in offset planes are not the same due to 3-dimensionality of the flow field.

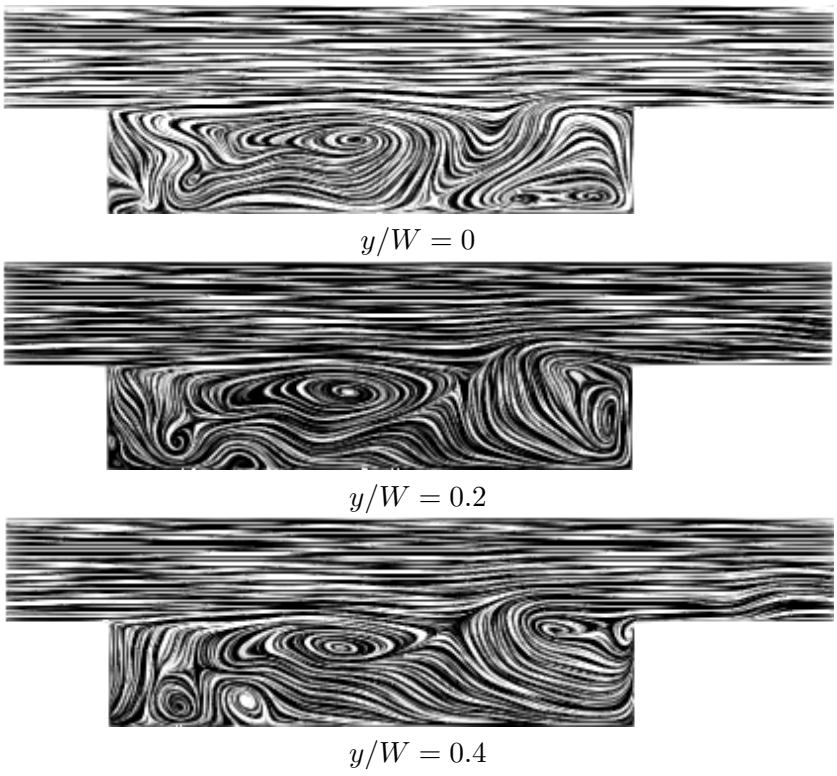

Figure 11: Instantaneous spanwise line integral convolution (LIC) images at offset planes

The cavity front and aft walls flow visualizations are also shown in Fig. 12 that demonstrates the existence of spanwise flow components clearly. Shear layer re-attachment and flow interactions around the cavity aft wall cause relatively more intense vortex structures around the trailing edge of the cavity.

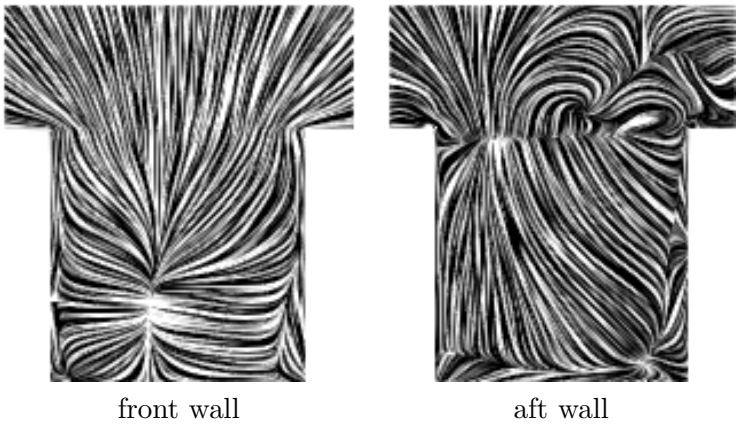

Figure 12: Instantaneous streamwise line integral convolution (LIC) images

In this respect, Fig. 13 demonstrates OASPL distributions at spanwise offset locations corresponding to $y/W = 0$ (centerline), $y/W = 0.2$ and $y/W = 0.4$ over the cavity front wall, ceiling and aft wall.

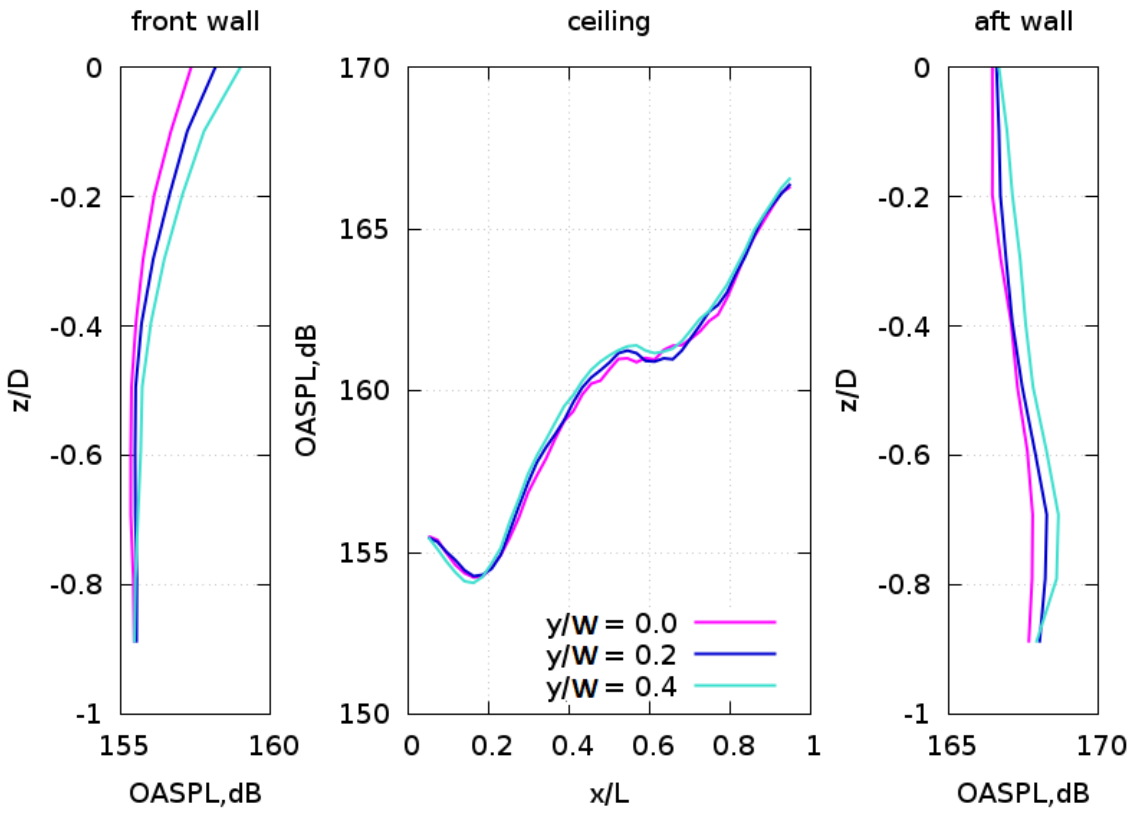

Figure 13: OASPL along $y/W = 0$, $y/W = 0.2$, and $y/W = 0.4$ over the front wall, ceiling and aft wall of the cavity

The results indicate that OASPL gets higher towards the cavity opening, i.e. $z = 0$, in the front wall of the cavity. As the offset distance increases from the cavity centerline (i.e. $y = 0$), noise intensity appears to increase around the cavity opening. Offset effects tend to disappear towards the cavity ceiling and OASPL is almost constant from $z/D = -0.6$ to the ceiling, as illustrated in Fig. 13 (left). On the other hand, noise intensity almost stays constant at various offset locations considered as shown in Fig. 13 (center). As it is expected, noise intensity increases significantly towards the aft wall of the cavity. This is caused mainly by the shear layer attachment on the cavity aft wall. Accompanying feedback mechanism also develops within the cavity that triggers intense noise around this region.

Noise intensity at the aft wall of the cavity also has negligible sensitivity to spanwise offset locations as illustrated in Fig. 13 (right). Vertical variation of noise intensity along the cavity aft wall is also not substantial.

OASPL distribution over the symmetry plane of the cavity is also computed and the results are provided in Fig. 14. It can be observed from the figure that noise intensity around the cavity aft wall is higher as expected due to highly unsteady shear layer attachment on the aft wall. Therefore, aft wall region of an internal weapon bay requires careful placement of internal instrumentation during the design because of high noise intensity.

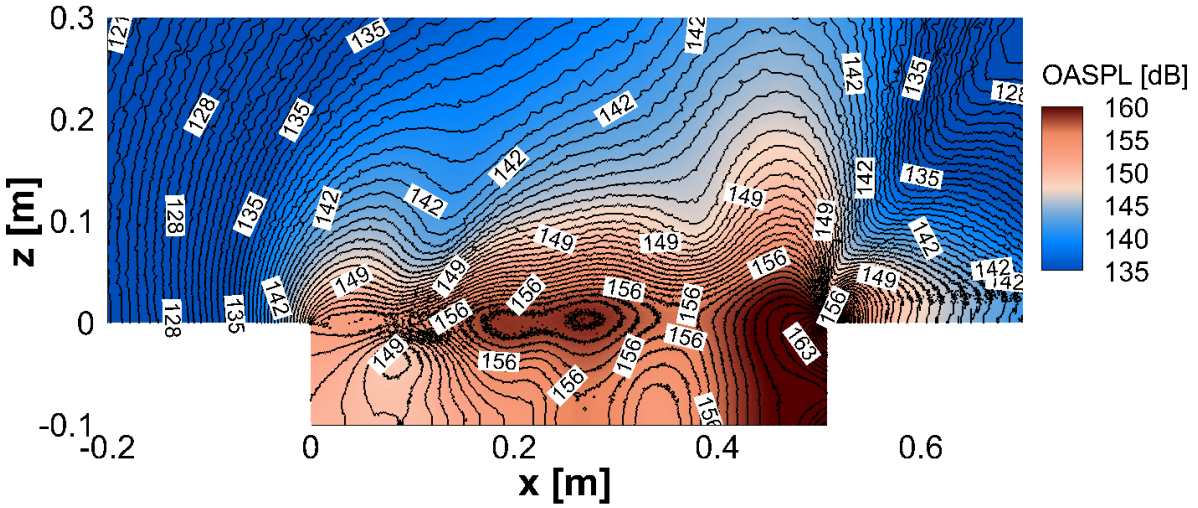

Figure 14: OASPL over the symmetry plane ($y/W = 0$) of the clean cavity

CONCLUSIONS

In this paper turbulent flow over the M219 clean cavity geometry at a Mach number of 0.85 and Reynolds number of 6.7×10^6 was predicted through URANS and DES computations using both RNG $k-\epsilon$ and $k-\omega$ SST URANS models and DES, DDES and IDDES methods. Various grid resolutions were tested to see the effects of grid resolution in URANS solutions both in the vicinity of the walls and in the cavity volume itself. Data collected at various locations along the centerline of the cavity ceiling were plotted against each other and experimental data. Increased grid resolution had minimal effects on the $k-\epsilon$ results, while the $k-\omega$ results improved significantly with the resolutions in the vicinity of the walls and in the cavity. Both had their own distinct effects. Although the URANS results had a bias in the computed cavity ceiling fluctutations in comparison to experimental data, it was shown in this study that both $k-\omega$ and $k-\epsilon$ methods can provide valuable SPL predictions for a configuration like the M219 clean cavity geometry. Modal frequencies of the cavity fluctuations are also sufficiently approximated. IDDES method among the other DES methods provided the best results for the current problem. IDDES captured OASPL along the centerline of cavity ceiling and pressure spectrum both in terms of frequencies and amplitudes of modes. IDDES proved its superiority over URANS models and it is considered as the appropriate solution method for cavity flows.

References

Barakos, G.J. (2018) *Understanding Transonic Weapon Bay Flows*, 7th European Conference on Computational Fluid Dynamics (ECFD 7). Glasgow,UK, 2018

Colonius, C.W. and Rowley and Basu, J.A.J. (2002) *On Self-sustained Oscillations in Two-dimensional Compressible Flow over Rectangular Cavities*, Fluid Mech, Vol 455, p: 315-346, 2002

ESDU (2004) *Aerodynamics and Aero-acoustics of Rectangular Planform Cavities: Part I: Time-averaged Flow*, ESDU, 2004

Kim, D.H. and Choi, J.H. and Kwon, O.J. (2015) *Detached Eddy Simulation of Weapons Bay Flows and Store Separation*, International Journal of Aeronautical and Space Sciences, Vol 16, p: 19-27, 2015

Lawson, S. and Barakos, G. (2011) *Review of Numerical Simulations for High-speed, Turbulent Cavity Flows*, Progress in Aerospace Sciences, Vol 47, p: 186-216, 2011

Nayyar, P. and Barakos, G. and Badcock, K. (2005) *Analysis and Control of Weapon Bay Flows*, NATO RTO AVT, p: 24-28, 2005

Pereira, J.C.F. and Sousa, J.M.M. (1995) *Experimental and Numerical Investigation of Flow Osciallations in a Rectangular Cavity*, Journal of Fluid Engineering, Vol 117, p: 68-74, 1995

Plentovich, E. and Stallings, Jr.R. and Tracy, M. (1993) *Experimental Cavity Pressure Measurements at Subsonic and Transonic Speeds*, Technical Paper 3358, NASA, 1993

Rizzetta, D.P. and Visbal, M.R. (2015) *Large-Eddy Simulation of Supersonic Cavity Flow Fields Including Flow Control*, International Journal of Aeronautical and Space Sciences, Vol 16, p: 19-27, 2015

Ross, J.A. and Peto, J.W. (1997) *The Effect of Cavity Shaping, Front Spoilers and Ceiling Bleed on Loads Acting on Stores, and on the Unsteady Environment Within Weapon Bays*, 1997

Rossiter, J.A. (1960) *A Preliminary Investigation into Armament Bay Buffet at Subsonic and Transonic Speeds*, Technical Memorandum AERO 679 Royal Aircraft Establishment, Aug 1960

Stallings, R.L.Jr. and Wilcox, F.J.Jr. (1960) *Experimental Cavity Pressure Distributions at Supersonic Speeds*, NASA TP-2683, 1960

Xiao, Z. and Luo, K. (2018) *Application of the IDDES Detached Eddy Simulation to Transonic and Supersonic Cavity Flows*, 2018

Zhang, X. and Edwards, J.A. (1990) *An Investigation of Supersonic Cavity Flows Driven by Thick Shear Layers*, Aeronautical Journal, Vol 94, p: 355-364, 1990

Ross, J. A. and Peto, J. W. (1997) *The Effect of Cavity Shaping, Front Spoilers and Ceiling Bleed on Loads Acting on Stores, and on the Unsteady Environment Within Weapon Bays*, QinetiQ, 1997